A P_N SPREADING MODEL CONSTRAINED WITH OBSERVED AMPLITUDES IN ASIA

Xiaoning (David) Yang

Los Alamos National Laboratory

Sponsored by the National Nuclear Security Administration

Award No. DE-AC52-06NA25396/LA09-IRP-NDD02

ABSTRACT

By modeling synthetic Pn amplitudes in 2007, my colleagues and I proposed a Pn geometric-spreading model (Y2007) that takes into account the spherical shape of the Earth. In this study, we used a set of observed Pn amplitudes from the tectonically active regions of Asia to evaluate the performance of Y2007 and to develop new, observation-based Pn spreading models. Even though Y2007 provides improved geometric-spreading correction of Pn amplitudes over the traditional power-law model, the corrected amplitudes exhibit undesirable decay-rate variations. To address this issue, we used a procedure to develop Pn spreading models based on observed data. We first correct the Pn amplitudes for attenuation using an average quality factor Q estimated from Y2007-corrected Pn amplitudes. We then develop a spreading model, which is a simplified version of Y2007, by fitting the corrected amplitudes. Compared with Y2007, the new spreading model significantly reduces amplitude variations, particularly at short distances. To more accurately model the complex data behavior, we also developed a segmented spreading model in which separate sets of model parameters are derived for amplitudes in different distance ranges. The spreading models developed in this study account for radially symmetric elastic and other effects, such as velocity gradient, forwarding scattering and potential depth-dependent attenuation variation, as well as geometric wavefront expansion and the spherical shape of the Earth. Using the new model for spreading correction results in better attenuation isolation and allows amplitudes in a broader distance range to be used in the accurate mapping of lateral attenuation variations. The method we employed in this study could be used as a general procedure to develop observation-based Pn spreading models for other regions.

Report Documentation Page

Form Approved
OMB No. 0704-0188

1. REPORT DATE	2. REPORT TYPE	3. DATES COVERED
SEP 2011		**00-00-2011 to 00-00-2011**

4. TITLE AND SUBTITLE	5a. CONTRACT NUMBER
A Pn Spreading Model Constrained with Observed Amplitudes in Asia	5b. GRANT NUMBER
	5c. PROGRAM ELEMENT NUMBER
6. AUTHOR(S)	5d. PROJECT NUMBER
	5e. TASK NUMBER
	5f. WORK UNIT NUMBER
7. PERFORMING ORGANIZATION NAME(S) AND ADDRESS(ES)	8. PERFORMING ORGANIZATION REPORT NUMBER
Los Alamos National Laboratory,P.O. Box 1663 ,Los Alamos,NM,87545	
9. SPONSORING/MONITORING AGENCY NAME(S) AND ADDRESS(ES)	10. SPONSOR/MONITOR'S ACRONYM(S)
	11. SPONSOR/MONITOR'S REPORT NUMBER(S)

12. DISTRIBUTION/AVAILABILITY STATEMENT

Approved for public release; distribution unlimited

13. SUPPLEMENTARY NOTES

Published in the Proceedings of the 2011 Monitoring Research Review - Ground-Based Nuclear Explosion Monitoring Technologies, 13-15 September 2011, Tucson, AZ. Volume I. Sponsored by the Air Force Research Laboratory (AFRL) and the National Nuclear Security Administration (NNSA). U.S. Government or Federal Rights License

14. ABSTRACT

By modeling synthetic Pn amplitudes in 2007, my colleagues and I proposed a Pn geometric-spreading model (Y2007) that takes into account the spherical shape of the Earth. In this study, we used a set of observed Pn amplitudes from the tectonically active regions of Asia to evaluate the performance of Y2007 and to develop new observation-based Pn spreading models. Even though Y2007 provides improved geometric-spreading correction of Pn amplitudes over the traditional power-law model, the corrected amplitudes exhibit undesirable decay-rate variations. To address this issue, we used a procedure to develop Pn spreading models based on observed data. We first correct the Pn amplitudes for attenuation using an average quality factor Q estimated from Y2007-corrected Pn amplitudes. We then develop a spreading model, which is a simplified version of Y2007, by fitting the corrected amplitudes. Compared with Y2007, the new spreading model significantly reduces amplitude variations, particularly at short distances. To more accurately model the complex data behavior, we also developed a segmented spreading model in which separate sets of model parameters are derived for amplitudes in different distance ranges. The spreading models developed in this study account for radially symmetric elastic and other effects, such as velocity gradient, forwarding scattering and potential depth-dependent attenuation variation, as well as geometric wavefront expansion and the spherical shape of the Earth. Using the new model for spreading correction results in better attenuation isolation and allows amplitudes in a broader distance range to be used in the accurate mapping of lateral attenuation variations. The method we employed in this study could be used as a general procedure to develop observation-based Pn spreading models for other regions.

15. SUBJECT TERMS

16. SECURITY CLASSIFICATION OF:			17. LIMITATION OF ABSTRACT	18. NUMBER OF PAGES	19a. NAME OF RESPONSIBLE PERSON
a. REPORT **unclassified**	b. ABSTRACT **unclassified**	c. THIS PAGE **unclassified**	**Same as Report (SAR)**	**11**	

Standard Form 298 (Rev. 8-98)
Prescribed by ANSI Std Z39-18

OBJECTIVES

The objective of the research is to develop accurate Pn geometric-spreading models from observed amplitudes to be used in tomographic inversions to map the lateral Pn attenuation variation.

RESEARCH ACCOMPLISHED

Introduction

It has long been recognized that the geometric spreading of the Pn wave in a spherical Earth is anything but the geometric spreading of a conical head wave (Červený and Ravindra, 1971; Hill, 1973; Sereno and Given, 1990; Yang et al., 2007). To account for the spherical shape of the Earth, Yang et al. (2007) proposed a new Pn geometric-spreading model based on synthetic simulations of Pn propagation in a spherical Earth model. The new model, abbreviated as Y2007 hereafter, is expressed as

$$G(r, f) = \frac{10^{n_3(f)}}{r_0}\left(\frac{r_0}{r}\right)^{n_1(f)\log_{10}\left(\frac{r_0}{r}\right)+n_2(f)} \qquad (r_0 = 1 \text{ km}) \tag{1}$$

and

$$n_i(f) = n_{i1}\left[\log_{10}\left(\frac{f}{f_0}\right)\right]^2 + n_{i2}\log_{10}\left(\frac{f}{f_0}\right) + n_{i3} \quad (i = 1, 2, 3;\ f_0 = 1 \text{ Hz}), \tag{2}$$

where r is epicentral distance and f is frequency. Although the Earth model that Yang et al. (2007) used for simulation was simple, the Pn spreading model that Yang et al. (2007) developed provides improved representation of the Pn propagation in the real Earth over the traditional power-law model. Using the new model to correct a set of observed Pn amplitudes for geometric spreading, Yang et al. (2007) obtained physically reasonable attenuation estimates at multiple frequencies from 0.75 to 6.0 Hz. Applying power-law geometric-spreading correction to the same dataset using a commonly assumed model, however, resulted in quality factor Q estimates that were either negative or too large (Yang et al., 2007).

In this study, we used a set of Pn amplitude measurements from 7,125 crustal earthquakes (depth ≤ 50 km) recorded by 27 seismic stations in Asia to evaluate the performance of Y2007. The evaluation shows that Y2007 provides satisfactory geometric-spreading corrections for amplitudes within limited distance range from 550 km to about 1400 km. Amplitude residuals, however, exhibit undesirable variations outside of the range. To better constrain Pn propagation in Asia, we developed new Pn spreading models by fitting observed Pn amplitudes. The new models account for not only the geometric wavefront expansion and the spherical shape of the Earth, but also other radially symmetric effects such as velocity gradient in the uppermost mantle and forward scattering. One of the main motivations to develop such spreading models is to provide a better spreading correction for Pn amplitudes that will be used to map lateral Pn attenuation variation. By removing spreading as well as other radially symmetric effects from Pn amplitudes, the new models better isolate the attenuation effect and render the resulting 2D Pn attenuation maps more accurate. In addition, bias caused by some radially symmetric effects is removed and amplitudes for a wider range of distances can be used in the attenuation tomography.

Pn Amplitudes

We collected a set of broadband, vertical-component seismograms for amplitude measurement. After converting the raw seismograms to ground displacements by removing the instrument response, we band-pass filtered the seismograms for a set of frequency bands from 0.5 Hz to 8 Hz and measured Pn root-mean-square (RMS) amplitudes from filtered waveforms. We then calculated pseudo-spectral amplitudes from the RMS amplitudes using the Parseval's-theorem-based method of Taylor, et al. (2002). These pseudo-spectral amplitudes were later used in the evaluation of Y2007 and in the development of the new spreading models. We used analyst P-wave pick t_p reported in earthquake catalogs to locate the time window for cutting Pn waveforms after filtering. The window starts at $t_1 = t_p$-0.0015r and ends at $t_2 = t_p$+0.0081r, where r is epicentral distance in kilometers. t_p, t_1 and t_2 are in seconds. This is a constant-velocity window and the length of the window thus defined is based on wave velocities 7.6 and 8.2 km/s. To select reliable measurements, we required that the Pn phase have an analyst pick and the

signal-to-noise ratio (SNR) be equal to or larger than 2. The requirement of an analyst pick and a large enough SNR appears to result in a set of high-quality amplitude measurements.

To isolate the path effect including spreading and attenuation, source and site-response effects need to be removed from the amplitudes, or to be accounted for. We removed the source effect using the Magnitude and Distance Amplitude Correction (MDAC) procedure (Walter and Taylor, 2001; Taylor et al., 2002). In MDAC, the source spectrum is represented by a Brune's (1970) earthquake model:

$$S(f) = \frac{M_0 R}{4\pi(\rho_s \rho_r v_s^5 v_r)^{1/2}[1 + (f / f_c)^2]} \quad (3)$$

where f is frequency; M_0 is source moment; R is source radiation factor; ρ is density; v is velocity and f_c is corner frequency. Subscripts s and r denote values for source and receiver regions, respectively. Taylor et al. (2002) derived a relationship between body-wave magnitude m_b and source moment M_0. We used the formula along with catalog m_b to calculate M_0 used in equation (3). We also adopted the elastic parameters, including velocity and density, used by Taylor et al. (2002) for a central Asia dataset in my calculation. We assumed an average P-wave source radiation factor of 0.44 (Boore and Boatwright, 1984). This simplification was adopted because of the lack of source-mechanism information. Since we used a large number of earthquakes with different radiation patterns, and for many of the earthquakes Pn amplitudes were measured at different azimuths, presumably, errors introduced by this simplification should be somewhat random and would unlikely affect the average amplitude behavior systematically. My experience with analyzing surface waves indicates that when amplitude measurements made at different azimuths and from a large number of earthquakes are used collectively, accurate compensation of the source radiation pattern may not be critical in certain applications (Yang et al., 2004). Because the stations we used are distributed over a large area with different site conditions, we assumed that the site responses would cancel out when the average amplitude trend is calculated.

Asia is a vast and tectonically diverse region. Some studies address the diversity by dividing the region into sub-regions based on their tectonic characteristics (Santô, 1965; Yacoub and Mitchell, 1977; Patton, 1980). In studying the phase velocity and attenuation of Rayleigh waves, Patton (1980) divided the Eurasia continent into five provinces. Figure 1 is a map of Asia showing the five provinces that Patton (1980) defined and the distribution of earthquakes and stations, from which we collected my data. According to Patton (1980), the "tectonic" province was defined as an area with its crustal thickness greater than 45 km or its elevation in excess of 1 km. The region does not include the Tibetan Plateau because of its unique crustal and upper-mantle structure. For the Tibetan Plateau, a "plateau" province was defined as the region with a Moho depth deeper than 55 km. The "platform" and "shield" provinces encompass the northern Eurasia platforms and the India Shield. These provinces are tectonically stable regions. Finally, the "plains" province was defined as areas with a crustal thickness thinner than 35 km. Patton (1980) characterized this province as a transitional province from continental to oceanic regions. The "tectonic" province plus the Tibetan Plateau approximately coincides with the largest "orogen" on the Earth identified by Bird (2003).

Due to different crustal and upper-mantle structure and material property between different provinces, Pn waves propagating in these regions may have different spreading and attenuation characteristics. For this reason, we divided my amplitude measurements into different groups for different provinces according to source and station locations. The criterion for the grouping was that when larger than about 90% of a Pn path is within a certain province, the corresponding amplitude was assigned to the group for that province. Owning to the size of and the large number of earthquakes and stations in the "tectonic" province, the majority of paths are in that province. The number of measurements in this group is about 65% of the total number of measurements. By contrast, 18% of the measurements are in the "plateau" group, 13% in the "plains" group, 2% in the "platform" group and 2% in the "shield" group. In the following sections, we will focus my analysis on Pn amplitudes for the "tectonic" province. By restricting my analysis to a single region with similar tectonic characteristics, the magnitude of large-scale spatial structure and material-property variations is minimized and it is more meaningful to discuss the concept of average spreading and attenuation for the region. The general procedure we followed may also be applied to other regions. To illustrate the amplitude behavior, Figure 2 plots the source-corrected amplitudes from the "tectonic" province as a function of epicentral distance at several frequencies. The amplitudes show considerable scatter around a general decay trend. Possible reasons for the scatter include lateral upper-mantle elastic and anelastic heterogeneities, source

error and site response variations. Despite the scatter, the mean amplitude decay should reflect mainly the average spreading and attenuation, which result from average or radially symmetric effects in the uppermost mantle of the "tectonic" province.

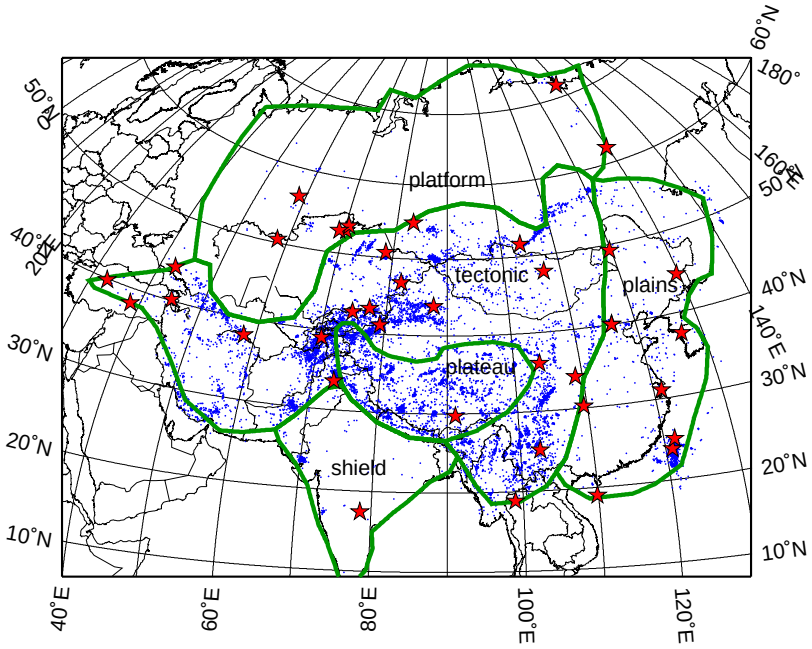

Figure 1. A map of Asia showing the five provinces defined by Patton (1980) based on crustal and upper-mantle structures. Also plotted are distributions of events (blue dots) and stations (red stars) that provided data for this study.

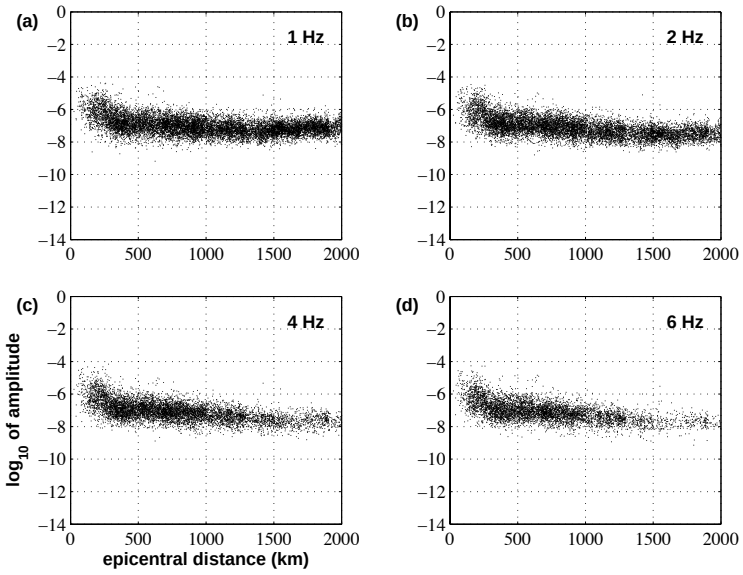

Figure 2. Source-corrected Pn amplitudes at 1, 2, 4 and 6 Hz. The amplitude decay as a function of distance is a combination of spreading and attenuation effects.

Geometric-Spreading Model Evaluation

To evaluate the performance of Y2007 in providing adequate corrections to observed Pn amplitudes, we removed the geometric-spreading effect from source-corrected amplitudes for the "tectonic" province using Y2007 and

analyzed the amplitude residuals. As an example, Figure 3 plots the 1-Hz source- and spreading-corrected Pn amplitudes as a function of distance. If the attenuation is constant, theoretically, after source and geometric-spreading corrections, the average of the logarithm of the amplitudes should be linearly related to distance (e.g., Aki and Richards, 2002; Box 5.7). Figure 3 shows that this is approximately true only in a limited range, i.e., between the two blue dashed lines marking the distances of 550 and 1400 km.

Beyond 1400 km, the deviation of the amplitude decay from the linear trend may be due to the well-known upper-mantle triplication phenomenon in which reflected waves from the 410- and 660-km discontinuities arrive at about the same time as Pn, thus contaminating the amplitude measurements. The reason for the amplitude decay-rate change below 550 km, however, is more difficult to isolate. Potential reasons for the variation include velocity gradient and forward scattering. If the top portion of the uppermost mantle has a predominantly positive velocity gradient and the rest on average has a constant P-wave velocity for the region, the overall effect would be to reduce the average decay rate of mainly short-distance Pn amplitudes. In addition, a distribution of scatterers in the uppermost mantle, or in the lower crust, could also result in the change of Pn amplitude decay rate through forward scattering (Tittgemeyer et al., 2000; Avants et al., 2011; Nielsen et al., 2003). The strong roll-off of amplitudes toward shorter distance below about 200 km is likely caused by Y2007 not being able to model short-distance amplitudes. The model was derived using synthetic data beyond 300 km (Yang et al., 2007). Amplitudes below 150 km may be contaminated or overtaken by Pg.

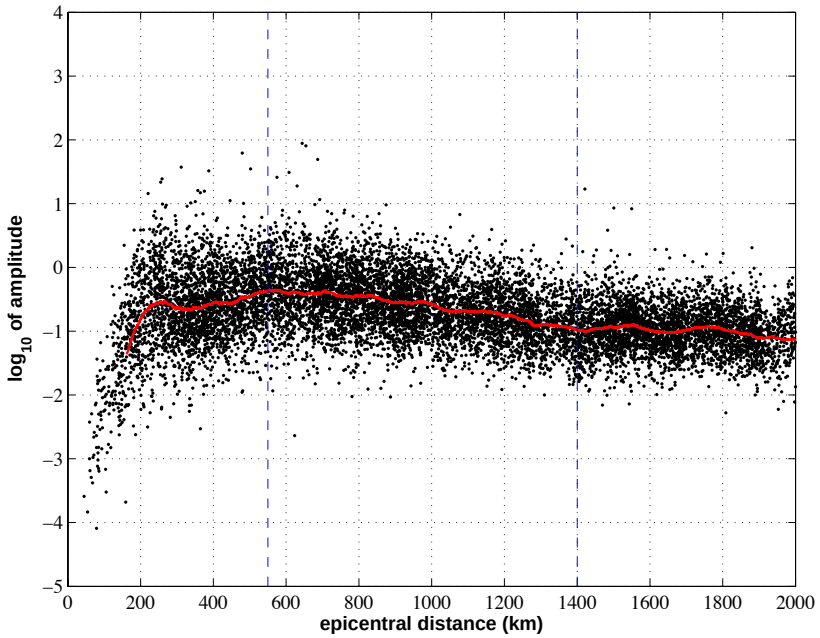

Figure 3. 1-Hz Pn amplitudes after source and geometric-spreading correction. The red line is the 400-point moving average indicating the average decay trend of the amplitudes.

Besides the amplitude-decay variations outside of the distance range from 550 to 1400 km, amplitudes within this range do not follow a perfectly constant decay rate either. One of the potential reasons for the decay-rate variation is the possible variation of attenuation with depth. The most significant attenuation change in the upper 200 km of the mantle occurs between the low-attenuation uppermost mantle and the high-attenuation asthenosphere (e.g., Dalton et al., 2008). To investigate the potential effect of the asthenosphere on Pn amplitudes, we calculated Pn penetration depths below the Moho for different distances based on ray geometry and the Earth model used by Yang et al. (2007). My calculation shows that for an uppermost mantle with no velocity gradient, the penetration depth for an epicentral distance of 550 km is 5 km. The penetration depth does not reach 35 km, which is the uppermost-mantle (mantle lid) thickness of the velocity model for the "tectonic" province specified by Patton (1980), until 1400 km distance. Furthermore, Pn Q estimated from the amplitude decay between 550- and 1400-km distances is larger than the asthenosphere P-wave Q (Qp) that we calculated from mantle S-wave Q (Qs) profiles of Hwang and Mitchell (1987) and Dalton et al. (2008). The above analysis indicates that although a low-Q asthenosphere may influence the

decay of Pn amplitudes, it may not be a significant contributor at least within 1400-km distance for the "tectonic" velocity structure (Patton, 1980).

An Observation-Based Pn Spreading Model

It appears that Y2007 is adequate for removing geometric, elastic and other radially symmetric effects from the amplitudes only within a limited distance range. In order to improve upon this, we developed a revised Pn spreading model based on Y2007 and measured Pn amplitudes for the "tectonic" province in Asia (Figure 1). The approach we employed was to first correct the source-corrected Pn amplitudes (Figure 2) with Y2007. We then estimated an average Q from the decay rate of the corrected amplitudes within the distance range where the amplitudes exhibit a linear trend against distance—the distance range between 550 and 1400 km marked by the two blue dashed lines in Figure 3. After obtaining the average Q, we corrected the source-corrected amplitudes (Figure 2) for attenuation using these average values. Finally, we used a simplified version of Y2007 to fit these corrected amplitudes and derived an observation-based Pn spreading model. The assumptions behind this approach are that the amplitude decay within the distance range between 550 and 1400 km is the result of apparent attenuation, and the Q estimated from the linear decay is representative of the average attenuation for the region. Based on the linear decay trend of the amplitudes, which is consistent with the theory of a constant Q effect, and the definition of the "tectonic" province as a tectonically active region with similar crustal and upper-mantle structure in most parts of the region, these assumptions seem reasonable.

Table 1 lists the average Pn Q we obtained by fitting source- and spreading-corrected amplitudes (Figure 3), along with the corresponding frequency bands. f_{desig} in Table 1 is the designated frequency that we use to refer to the frequency bands. f is the frequency of the source and average-attenuation corrected amplitudes that we later used to fit the new spreading model. This frequency is calculated as $f = \sqrt{f_l f_h}$ where f_l and f_h are the lower and higher limits of the corresponding frequency band (Bowman and Kennett, 1991; Hartse et al., 1997).

Table 1. Average *Q* Estimated from Source and Geometric-spreading Corrected Amplitudes and Corresponding Frequency Bands

f_{desig} (Hz)	0.5	0.75	1.0	1.25	1.5	2.0	2.5	3.0	4.0	6.0	8.0
f **(Hz)**	0.71	1.06	1.41	1.77	2.12	2.83	3.54	4.24	4.90	6.93	8.94
band	0.5-1.0	0.75-1.5	1.0-2.0	1.25-2.5	1.5-3.0	2.0-4.0	2.5-5.0	3.0-6.0	4.0-6.0	6.0-8.0	8.0-10.0
Q	635	381	326	321	329	362	412	465	519	618	743

The Q values that we obtained are generally consistent with published P-wave Q estimates for Asia. For example, Sereno (1990) used Pn amplitude spectra to invert for Q for eastern Kazakhstan in central Asia. One of his Q models from the inversion produces Q values between 253 and 897 for frequencies between 0.71 and 8.94 Hz. Although Sereno (1990) used a power-law model for geometric-spreading correction, because the power-law model yields a similar average path correction as that from Y2007 in the distance range (< 1000 km) of the data that he used (Sereno, 1990; Figure 4), the resulting Q should be comparable to what we obtained in this study. In another study, Der et al. (1986) estimated P-wave Q under the northern Eurasian shield using teleseismic body waves. They obtained Q values between about 600 and 1500 for frequencies between 0.3 and 10 Hz at depths between 0 and 100 km below the surface. These values should be near the upper bound of uppermost-mantle P-wave Q in Asia.

After obtaining the average Q, we removed the attenuation effect from the source-corrected Pn amplitudes (Figure 2) using these values. The average behavior of the resulting amplitude residuals should then reflect only the geometric spreading and other possible elastic and radially symmetric effects, and can be used to fit a spreading model that better describes the effects. As an example, Figure 4 shows the 1-Hz source and attenuation corrected Pn amplitudes. The red line is the 400-point moving average.

The model we developed by fitting observed amplitudes is a simplified version of Y2007. From the amplitude-residual behavior shown in Figure 4, it is apparent that because of the curvature of the moving average, particularly at short distances, at least a quadratic function of log(distance) is needed to better fit the data for the whole distance range from 150 to 1400 km. We then used the same distance-dependence function of Y2007 (Eq. 1) for the new spreading model. The coefficients n_i of the new model, however, depend linearly on the logarithm of frequency as in

$$n_i = n_{i1} \log_{10}\left(\frac{f}{f_0}\right) + n_{i2} \qquad (i = 1, 2, 3;\ f_0 = 1\ \text{Hz}). \qquad (4)$$

This functional form was chosen based on the behavior of n_i, which were derived from fitting amplitudes to Eq. (1) at individual frequencies, as a function of frequency. Using a quadratic frequency dependence (Eq. 2) with a larger number of model parameters yielded essentially the same result in terms of the overall shape of the model as a function of distance and frequency. Both parameterizations also have comparable prediction errors.

To derive the model parameters of the new observation-based Pn spreading model, we fit equations (1) and (4) to the source and average-attenuation corrected Pn amplitudes between 150 and 1400 km. The resulting model parameters are listed in Table 2.

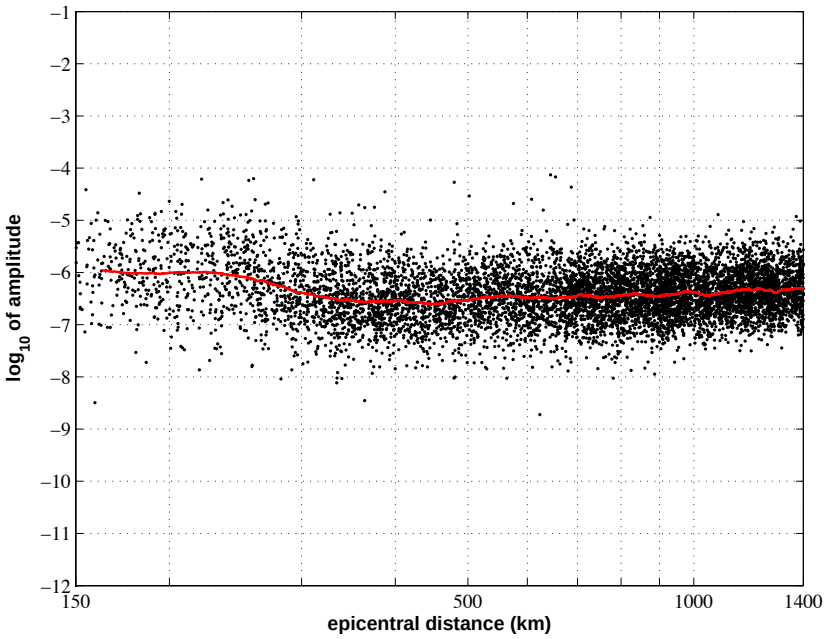

Figure 4. 1-Hz Pn amplitudes after source and average-attenuation correction. The red line is the 400-point moving average of the amplitudes.

To demonstrate the improvement of the new spreading model over Y2007 in isolating the attenuation effect, in Figure 5 we plot 1-, 2-, 4-, and 6-Hz Pn amplitudes after source and spreading correction using the new model. Also plotted in the figure are the 400-point moving average of either the amplitudes shown in the figure or those corrected with Y2007 (e.g., Figure 3). It is evident that the new model provides a much better spreading correction, particularly for short distances, in terms of residuals displaying a constant decay trend. Even though the model was developed using amplitudes below 1400 km, it yields reasonable path corrections for amplitudes at longer distances as well. Using the new spreading model and amplitudes between 150 and 1400 km, we obtained average Q values that are similar to the Q values listed in Table 1, which were obtained using data between more limited distance range between 550 and 1400 km.

Table 2. Parameters of the New P_n Spreading Model

n_{11}	n_{12}	n_{21}	n_{22}	n_{31}	n_{32}
1.520	1.636	6.228	9.379	6.308	6.861

A Segmented Spreading Model

Figure 3 shows that Pn amplitudes corrected for geometric spreading with Y2007 exhibit amplitude-decay variations in multiple distance ranges. The approach described in the previous section seeks to reduce these variations by fitting a single model to the amplitudes for the complete distance range. Figure 5 indicates that the model does a decent job reducing the most apparent decay-rate change at about 550 km. At short distances, however, some variations still exist. This is due to the limitation of using a single model with a simple functional form to fit the complex data behavior. One approach to address this issue is to use separate models for different distance ranges. We refer to such a model representation as the segmented model. Seismologists have used this approach to model the geometric-spreading of shear waves from earthquakes (e.g., Atkinson and Mereu, 1992; Boore, 2003). In fact, the standard power-law model of Street et al. (1975) is a form of segmented model.

To construct a segmented spreading model, we divided the whole distance range from 150 to 1400 km into two segments: between 150 and 340 km (first segment), and between 340 and 1400 km (second segment) based on the amplitude behavior (Figure 4). One can choose a variety of model formulations, e.g., the Y2007 formula or a power-law model, for the model segments. To keep the model parameterization consistent, we chose to use the same functional form of the single spreading model developed in the last section (Eqs. 1 and 4) for both model segments.

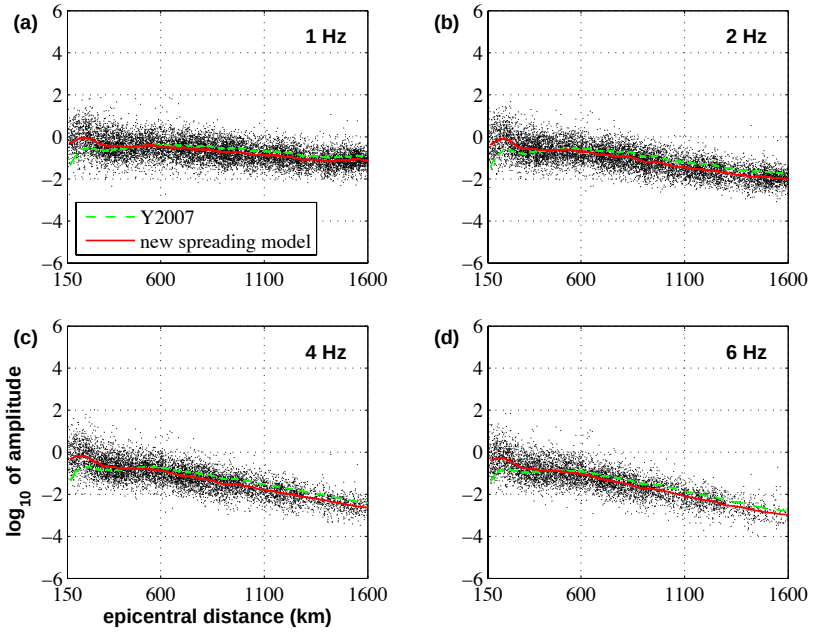

Figure 5. Pn amplitudes after source and spreading correction using the new model. Yellow lines are the 400-point moving average of the amplitudes. Green lines are the 400-point moving average of the amplitudes, which are not shown, corrected using Y2007.

Table 3 lists the model parameters of the segmented spreading model derived from fitting amplitudes in different distance segments. Figure 6 shows 1-, 2-, 4- and 6-Hz Pn amplitudes after source and spreading correction using the segmented model. Moving average of amplitudes corrected with either the segmented model or Y2007 are also plotted. Again, the segmented spreading model performs significantly better than Y2007. Compared with Figure 5, the segmented model further reduced amplitude variation about the constant decay trend, particularly at short distances.

Table 3. Parameters of the Segmented Spreading Model

Segment	n_{11}	n_{12}	n_{21}	n_{22}	n_{31}	n_{32}
first	3.811	-11.116	17.782	-50.961	20.777	-64.353
second	0.849	0.187	2.479	1.010	1.094	-5.188

To offer a clearer comparison between the segmented model and the single model developed in the previous section, we plot the moving average of 1-Hz Pn amplitudes corrected using either the single spreading model or the segmented model together in Figure 7. Also plotted in the figure is the moving average of amplitudes corrected with Y2007. Both single and segmented models perform much better than Y2007 in yielding amplitude residuals with constant decay rate, particularly below 550 km. The segmented model further reduces the large amplitude variations below 400 km compared with the single model. In addition, amplitude residuals from the segmented model also have a slightly smaller deviation from the constant decay around 600 to 800 km.

CONCLUSIONS AND RECOMMENDATIONS

Based on the Pn geometric-spreading model of Yang et al. (2007) (Y2007) for a simple spherical Earth model, we developed new Pn spreading models for the tectonically active regions of Asia, except the Tibetan Plateau, using a set of high-quality Pn amplitude measurements from 0.5 to 8 Hz. A single spreading model, which is similar to Y2007 but is simpler, from fitting observed amplitudes between 150 and 1400 km provides improved amplitude corrections for removing decay-rate variations, particularly for reducing the most apparent decay-rate change at about 550 km. Modeling different segments of the amplitudes with separate models proves to be even more effective, although it requires a more complex model representation. In addition to the geometric effect, these new models should also account for other radially symmetric effects, such as velocity gradients, and yield corrected amplitudes that more accurately reflect the anelastic attenuation property of the uppermost mantle and can be used to better constrain the lateral variation of the attenuation.

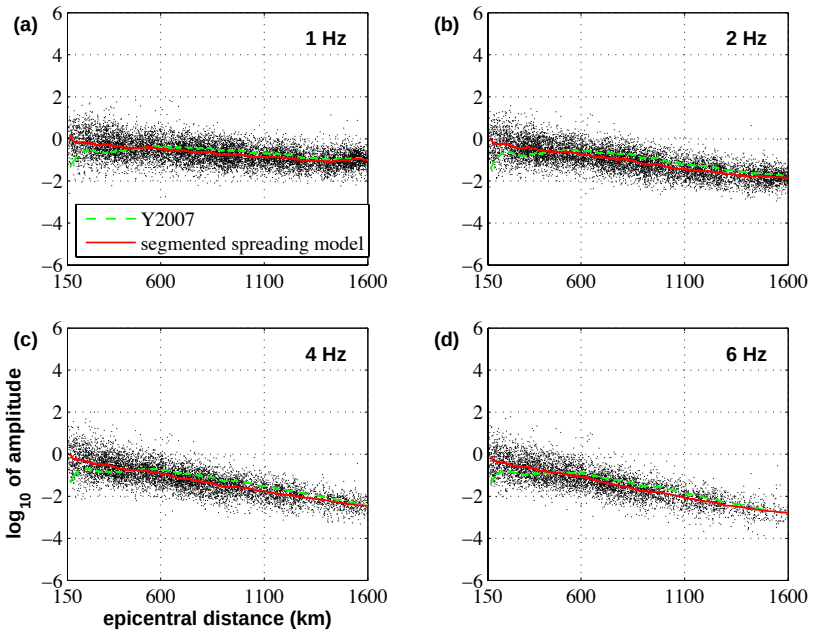

Figure 6. Same as Figure 5 but with amplitudes corrected using the segmented spreading model.

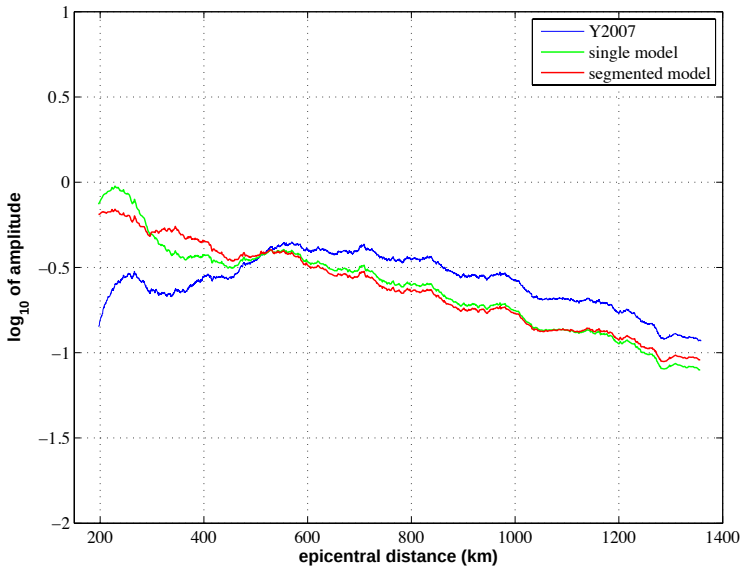

Figure 7. 400 Moving average of 1-Hz source and spreading corrected Pn amplitudes using either Y2007, the single spreading model, or the segmented spreading model.

ACKNOWLEDGEMENTS

Richard Stead of the Los Alamos National Laboratory collected all the seismograms and other metadata used in this study from IRIS/DMC and other sources, and put them in a comprehensive database, from which we made the amplitude measurements. He is instrumental in making sure that all data and information are accurate and free of error. I benefited greatly from discussions with Scott Phillips of the Los Alamos National Laboratory about the characteristics of Pn propagation in Asia. This study was stimulated by some of those discussions. Scott Phillips also generously provided his amplitude measurement code to me, which helped tremendously.

REFERENCES

Aki, K. and P. G. Richards (2002). *Quantitative Seismology*, 2nd ed. Sausalito: University Science Books.

Atkinson, G. M. and R. F. Mereu (1992). The shape of ground motion attenuation curves in southeastern Canada, *Bull. Seismol. Soc. Am.* 82: 2014–2031.

Avants, M., T. Lay, X.-B. Xie, and X. Yang (2011). Effects of 2D random velocity heterogeneities in the mantle lid and Moho topography on Pn geometric spreading, *Bull. Seismol. Soc. Am.* 101: 126–140, doi: 10.1785/0120100113.

Bird, P. (2003). An updated digital model of plate boundaries, *Geochem. Geophys. Geosyst*. 4: 1027, doi: 10.1029/2001GC000252.

Boore, D. M. and J. Boatwright (1984). Average body-wave radiation coefficients, *Bull. Seismol. Soc. Am*. 74: 1615–1621.

Boore, D. M. (2003). Simulation of ground motion using the stochastic method, *Pure App. Geophys*. 160: 635–676, doi: 10.1007/PL00012553.

Bowman, J. R. and B. L. N. Kennett (1991). Propagation of Lg waves in the North Australian Craton: Influence of crustal velocity gradients, *Bull. Seismol. Soc. Am*. 81: 592–610.

Brune, J. N. (1970). Tectonic stress and the spectra of seismic shear waves from earthquakes, *J. Geophys. Res*. 75: 4997–5009.

Červený, V. and R. Ravindra (1971). *Theory of Seismic Head Waves.* Toronto: University of Toronto Press.

Dalton, C. A., G. Ekström, and A. M. Dziewoński (2008). The global attenuation structure of the upper mantle, *J. Geophys. Res*. 113: B09303, doi: 10.1029/2007JB005429.

Der, Z. A., A. C. Lees, and V. F. Cormier (1986). Frequency dependence of Q in the mantle underlying the shield areas of Eurasia. III. The Q model, *Geophys. J. Roy. Astron. Soc*. 87: 1103–1112.

Hartse, H. E., S. R. Taylor, W. S. Phillips, and G. E. Randall (1997). A preliminary study of regional seismic discrimination in central Asia with emphasis on western China, *Bull. Seismol. Soc. Am*. 87: 551–568.

Hill, D. P. (1973). Critically refracted waves in a spherically symmetric radially heterogeneous earth model, *Geophys. J. Roy. Astron. Soc*. 34: 149–177.

Hwang, H. J. and B. J. Mitchell (1987). Shear velocities, Q_β, and the frequency-dependence of Q_β in stable and tectonically active regions from surface-wave observations, *Geophys. J. Roy. Astron. Soc*. 90: 575–613.

Müller, G. (1985). The reflectivity method: a tutorial, *J. Geophys*. 58: 153–174.

Nielsen, L., H. Thybo, I. B. Morozov, S. B. Smithson, and L. Solodilov (2003). Teleseismic Pn arrivals: influence of mantle velocity gradient and crustal scattering, *Geophys. J. Int*. 152: F1-7.

Patton, H. (1980). Crust and upper mantle structure of the Eurasian continent from the phase velocity and Q of surface waves, *Rev. Geophys*. 18: 605-625, doi: 10.1029/RG018i003p00605.

Santô, T. (1965). Lateral variation of Rayleigh wave dispersion character, Part II: Eurasia, *Pure App. Geophys*. 62: 67–80.

Sereno, T. J. and J. W. Given (1990). Pn attenuation for a spherically symmetric Earth model, *Geophys. Res. Lett*. 17: 1141–1144.

Sereno, T. J. (1990). Frequency-dependent attenuation in eastern Kazakhstan and implications for seismic detection thresholds in the Soviet Union, *Bull. Seismol. Soc. Am*. 80: 2089–2105.

Street, R. L., R. B. Herrmann, and O. W. Nuttli (1975). Spectral characteristics of the Lg wave generated by central United States earthquakes, *Geophys. J. Roy. Astron. Soc*. 41: 51–63, doi: 10.1111/j.1365-246X.1975.tb05484.x.

Taylor, S. R., A. A. Velasco, H. E. Hartse, W. S. Phillips, W. R. Walter, and A. J. Rodgers (2002). Amplitude corrections for regional seismic discriminants, *Pure App. Geophys*. 159: 623–650.

Tittgemeyer, M., F. Wenzel, and K. Fuchs (2000). On the nature of Pn, *J. Geophys. Res*., 105: 16173–16180.

Walter, W. R. and S. R. Taylor (2001). A revised Magnitude and Distance Amplitude Correction (MDAC2) procedure for regional seismic discriminants, Lawrence Livermore National Laboratory UCRL-ID-146882: http://www.llnl.gov/tid/lof/documents/pdf/240563.pdf

Yacoub, N. K. and B. J. Mitchell (1977). Attenuation of Rayleigh-wave amplitudes across Eurasia, *Bull. Seismol. Soc. Am*. 67: 751–769.

Yang, X., T. Lay, X.-B. Xie, and M. S. Thorne (2007). Geometric spreading of Pn and Sn in a spherical earth model, *Bull. Seismol. Soc. Am*. 97: 2053–2065, doi: 10.1785/0120070031.

Yang, X. N., S. R. Taylor, and H. J. Patton (2004). The 20-s Rayleigh wave attenuation tomography for central and southeastern Asia, *J. Geophy. Res*. 109: B12304, doi: 10.1029/2004JB003193.